NEW CRITERION FOR SHAPE OPTIMIZATION OF NORMAL-CONDUCTING ACCELERATOR CELLS FOR HIGH-GRADIENT APPLICATIONS*

Kyrre Ness Sjobak† and Erik Adli (Department of Physics, University of Oslo, Norway)
Alexej Grudiev (CERN, Geneva, Switzerland)

Abstract

When optimizing the shape of high-gradient accelerating cells, the goal has traditionally been to minimize the peak surface electric field / gradient, or more recently minimizing the peak modified Poynting vector / gradient squared. This paper presents a method for directly comparing these quantities, as well as the power flow per circumference / gradient squared. The method works by comparing the maximum tolerable gradient at a fixed pulse length and breakdown rate that can be expected from the different constraints. The paper also presents a set of 120° phase-advance cells for traveling wave structures, which were designed for the new CLIC main linac accelerating structure, and which are optimized according to these criteria.

INTRODUCTION

One of the main challenges for the Compact LInear Collider (CLIC) [1] is the design of accelerating structures which are able to reach very high gradients for long enough pulse lengths to efficiently produce useful amounts of luminosity. Part of this is done by optimizing the overall design of the structure, such as its length, aperture and tapering while obeying constraints from beam dynamics and minimizing the total cost of the machine [2]. An important component of these calculations is the fast estimation of the RF parameters and breakdown constraints of a candidate accelerating structure [3]. These estimates are based on a database of pre-calculated accelerator cell geometries for a large number of different iris apertures and thicknesses [4]. The optimization of these cell geometries for maximizing the gradient for a given breakdown rate is the topic of this paper.

QUANTITIES FOR OPTIMIZATION

Traditionally, accelerating cavities where optimized using constraints on the peak surface electric field $\hat{E}$ [5], peak surface magnetic field $\hat{H}$, or more recently power flow constraints such as the averaged power flow through the cell by the iris aperture circumference P/C [6] or the peak modified Poynting vector $\hat{S}_c$ [7]. While the geometry parameters affecting $\hat{H}$ is often mostly orthogonal to the other constraints, the choice of which of the iris-dominated constraints $\hat{E}$, P/C or $\hat{S}_c$ to optimize for produces different geometries, as demonstrated in the next section.

† k.n.sjobak@fys.uio.no

However, the iris-dominated constraints can be directly compared by using the observed scaling relation [7] for the average accelerating gradient G, pulse length τ and the breakdown rate BDR

$$\frac{G^{30}\tau^5}{\text{BDR}} = K \ , \tag{1}$$

where K is a scaling constant which varies between different structures. By scaling the achieved gradient G for different cavities to a set of standard conditions with breakdown rate $\text{BDR}_0 = 10^{-6}$ breakdowns / pulse / structure length in meter and pulse length $\tau_0 = 200$ ns, the achievable gradient G' can be directly compared between different cavities.

Further, using FEM simulations of the accelerating mode in a given geometry, it is possible to calculate the ratios between the limiting factors and the average accelerating gradient as $\bar{E} \equiv \hat{E}/G$, $\bar{S}_c \equiv \hat{S}_c/G^2$ and also $(P/C)/G^2$. These ratios are independent of the field level. The normalized peak fields can then be applied to the re-scaled gradient G', yielding a comparison of the peak fields at a common breakdown rate BDR_0 and pulse length τ_0, as shown in Fig. 1.

From the data presented in Fig. 1 and using Eq. 1, an expression for the *breakdown index*

$$\kappa \equiv K^{1/5} = \left(\frac{G^{30}\tau^5}{\text{BDR}}\right)^{1/5} = \frac{G^6\tau}{\text{BDR}^{1/5}} \tag{2}$$

can be defined for each of the limiting factors. For a given geometry, three breakdown indexes κ_E, κ_{S_c} and $\kappa_{P/C}$ can thus be computed and compared with the same dimensions. A higher value of κ implies that the cell is less likely to break down due to that peak field, and for optimization purposes, the worst (smallest) breakdown index is used, such that the overall value for the cell is given as

$$\kappa = \min\left(\kappa_E, \kappa_{S_c}, \kappa_{P/C}\right) \ . \tag{3}$$

In many cases, the breakdown index is easier to interpret when converted to a maximum gradient $\hat{G}$ at the standard conditions. This can be calculated as

$$\hat{G} = \frac{\kappa^{1/6} \, \text{BDR}_0^{1/30}}{\tau_0^{1/6}} \ . \tag{4}$$

For $\hat{E}$, the following scaling limit can be found

$$\kappa_E \bar{E}^6 = \frac{\hat{E}^6\tau}{\text{BDR}^{1/5}} \leq \frac{\hat{E}_0^6\tau_0}{\text{BDR}_0^{1/5}} \ , \tag{5}$$

where $\hat{E}_0$ is the peak field limit at standard conditions (220–250 MV/m), indicated with red lines in Fig. 1 [8]. When
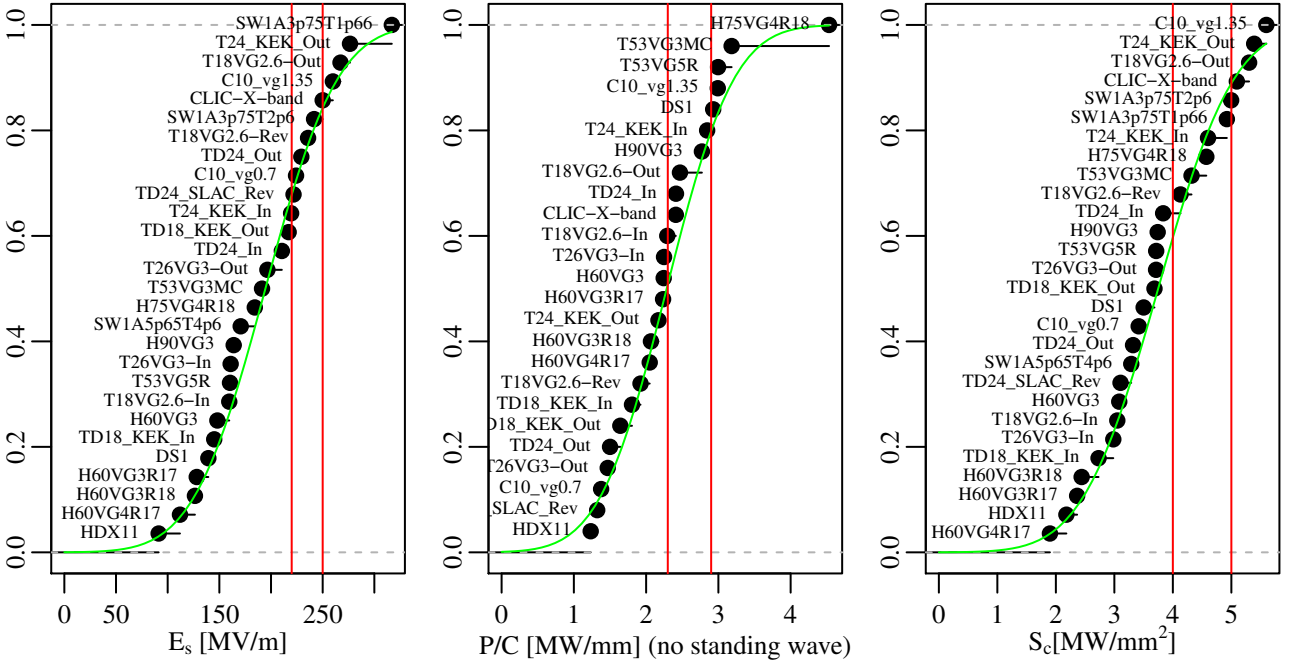
Figure 1: The maximum $\hat{E}$, P/C and $\hat{S}_c$ for a range of different tested accelerating structures, when the gradient for each structure is scaled to G' using Eq. 1 [8]. The curved green lines are the cumulative distribution functions for Gaussian distributions with μ and σ given by the mean and sample variance of the data. The vertical red lines are the chosen "pessimistic" and "optimistic" limits.

operating at the limit, the electric breakdown index can thus be written as

$$\kappa_E = \left(\frac{\hat{E}_0^6 \tau_0}{\mathrm{BDR}_0^{1/5}}\right) \cdot \frac{1}{\bar{E}^6} = \frac{\hat{G}_E^6 \tau_0}{\mathrm{BDR}_0^{1/5}} , \qquad (6)$$

where $\hat{G}_E$ is the maximum permitted gradient from the electric field when running at standard conditions, in a cell with normalized electric field $\bar{E}$.

For the peak modified Poynting vector $\hat{S}_c$, the relation is

$$\kappa_{S_c} \bar{S}_c^3 = \frac{\hat{S}_c^3 \tau}{\mathrm{BDR}^{1/5}} \leq \frac{\hat{S}_{c0}^6 \tau_0}{\mathrm{BDR}_0^{1/5}} , \qquad (7)$$

where $\hat{S}_{c0}$ is the peak field limit at standard conditions (4–5 MV/mm^2) [8]. The modified Poynting vector breakdown index can thus be written as

$$\kappa_{S_c} = \left(\frac{\hat{S}_{c0}^3 \tau_0}{\mathrm{BDR}_0^{1/5}}\right) \cdot \frac{1}{\bar{S}_c^3} = \frac{\hat{G}_{S_c}^6 \tau}{\mathrm{BDR}^{1/5}} , \qquad (8)$$

where $\hat{G}_{S_c}$ is the maximum permitted gradient from S_c when running at standard conditions, in a cell with normalized modified Poynting vector $\bar{S}_c$.

For P/C, a similar relation is also possible. For this, an expression for the gradient G as a function of the power flow P is needed. This can be shown to be given as

$$G^2 = \frac{P \omega R'/Q}{v_g} , \qquad (9)$$

where ω is the resonance frequency of the mode in radians per unit time, R' the shunt impedance per unit length, Q the

quality factor of the mode and v_g the group velocity. All of these are usually calculated as a function of the geometry parameters when designing a cell for a traveling wave structure. This leads to the relation

$$\kappa_{P/C} \left(\frac{v_g}{\omega R'/QC}\right)^3 = \frac{(P/C)^3 \tau}{\mathrm{BDR}^{1/5}} \leq \frac{(P/C)_0^3 \tau_0}{\mathrm{BDR}_0^{1/5}} , \qquad (10)$$

where $(P/C)_0$ is the limit at standard conditions (2.3–2.9 MW/mm). The P/C breakdown index is thus

$$\kappa_{P/C} = \frac{(P/C)_0^3 \tau_0}{\mathrm{BDR}_0^{1/5}} \left(\frac{\omega R'/QC}{v_g}\right)^3 = \frac{\hat{G}_{P/C}^6 \tau}{\mathrm{BDR}^{1/5}} , \qquad (11)$$

where $\hat{G}_{P/C}$ is the maximum permitted gradient from P/C when running at standard conditions, in a cell with the given values of ω, v_g and R'/Q .

OPTIMIZED ACCELERATOR CELLS

The main purpose of developing the method was to create a set of optimized accelerator cells for the CLIC re-baselining study [2]. The resulting cell designs span a range of iris aperture openings a and thicknesses d, typically normalized to the wavelength λ and cell length h. For each of the (a, d)-points, a 5-parameter optimization was used to find the optimum shape [4, 9]. The resulting gradient capability $\hat{G}$ at standard conditions is shown in Fig. 2. From this plot, the main trend is that the gradient capability drops off as the aperture increases. However, a structure consisting of purely small-aperture cells would not be practical, as the group velocity in these cells is very small.

03 Technology

3B Room Temperature RF
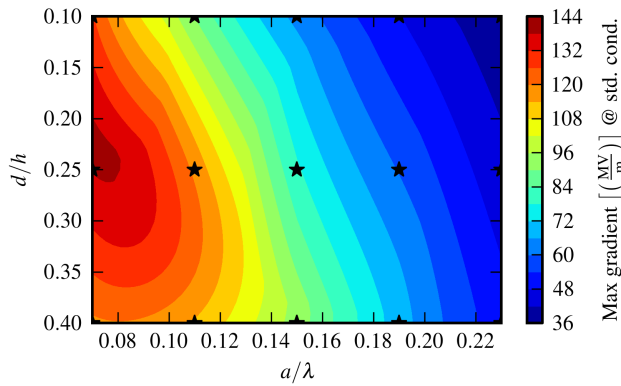
Figure 2: Estimated gradient capability $\hat{G}$ for finished cell designs. The plot shows a 2nd order interpolated surface, where the interpolation points (the stars in the plot) are taken from a database [4] of cells optimized for maximizing κ.
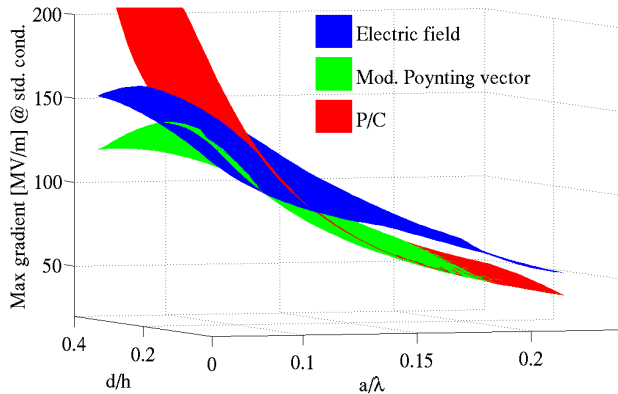
Figure 3: Estimated gradient capability for finished cell designs, as predicted from each of the three limits.

Fig. 3 shows the gradient capability of a cell as a function of the iris aperture and thickness, as predicted from each of the three limits. This shows that different limits are dominating for different apertures, with $\hat{E}$ and $\hat{S}_c$ both being important for small apertures, while for larger apertures $\hat{S}_c$ and P/C are dominating.

As illustrated in Fig. 4, in cells where multiple constraints are relevant, the constraints tend to favor different iris shapes. One example is the small-aperture cell $a/\lambda = 0.07$,
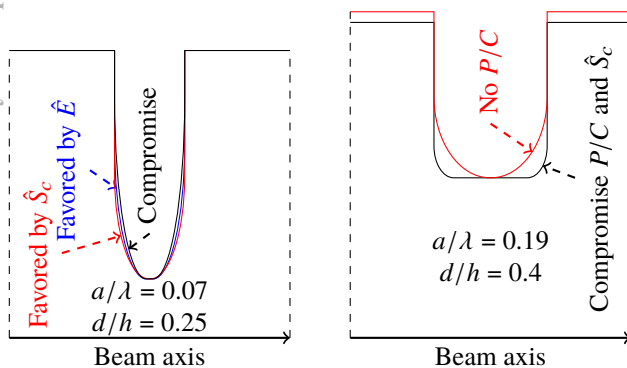
$d/h = 0.25$, where $\hat{E}$ and $\hat{S}_c$ are important. Here $\hat{E}$ avoids concentrating the electric field in a small area, while $\hat{S}_c$ tends to separate the electric- and magnetic surface fields, often at the cost of higher peak fields. Another example is cells with larger apertures, such as $a/\lambda = 0.19$, $d/h = 0.4$ where $\hat{S}_c$ and P/C are important. Here P/C favors very square irises which decreases the group velocity, reducing $\kappa_{P/C}$ at the cost of stronger peak fields. When optimizing the geometry of these cells, the breakdown index provides a method for directly comparing the importance of the different constraints, yielding an overall optimum.

DISCUSSION AND CONCLUSIONS

This paper presented a method for directly comparing breakdown constraints from $\hat{E}$, $\hat{S}_c$ and P/C, as well as it's use for optimizing a set of cells for high gradient performance.

One limitation of this method is the lack of uniformity in the data used for setting the limits $\hat{E}_0$, $\hat{S}_{c0}$ and $(P/C)_0$, and also the data's normalization for structure length when the fields in the structures is not likely to be uniform. However, given the large difference in the power which the gradient and BDR (and with it, the structure length) enter Eq. 1, the normalization is a relatively minor concern.

ACKNOWLEDGMENT

REFERENCES

[1] M. Aicheler, P. Burrows, M. Draper, T. Garvey, P. Lebrun, K. Peach, N. Phinney, H. Schmickler, D. Schulte, and N. Toge, editors. *A Multi-TeV linear collider based on CLIC technology: CLIC Conceptual Design Report, volume 1.* CERN, 2012.

[2] D. Schulte, "Status of CLIC parameter rebaselining studies". Presented at the 2014 CLIC workshop, CERN, Feb. 7th 2014.

[3] Kyrre Ness Sjobak. "The CLICopti RF structure parameter estimator". CLIC note 1031, CERN, 2014.

[4] K. Sjobak. "Design of waveguide damped cells for 12 GHz high gradient accelerating structures." CLIC note 1026, CERN, 2014.

[5] W.D.Kilpatrick. "Criterion for vacuum sparking design to include both rf and dc". *The review of scientific instruments*, 28(10):824–826, October 1957.

[6] W. Wuensch. "The scaling of the traveling-wave rf breakdown limit". CLIC note 649, CERN, January 2006.

[7] A. Grudiev, S. Calatroni, and W. Wuensch. "New local field quantity describing the high gradient limit of accelerating structures". *Phys. Rev. ST Accel. Beams*, 12:102001, Oct 2009.

[8] A. Grudiev. "RF constraints. Update 2013 for CLIC rebaselining". Presented at the 6th CLIC design meeting, April 19th 2013.

[9] Kyrre Ness Sjobak, Erik Adli, and Alexej Grudiev. "Surface field optimization of accelerating structures for CLIC using ACE3P on remote computing facility". In *Proceedings of IPAC2013*, Shanghai, China, 2013.

Figure 4: Iris shapes favored by different limiting factors.